

Premature Stiffening of Cement Paste Caused by Secondary Gypsum and Syngenite Formation (False Set)

Chul-Woo Chung and Jae-Yong Lee

Pacific Northwest National Laboratory, Richland, WA, USA

Department of Architectural Engineering, Pukyong National University, Nam-Gu, Busan, Korea

DOI: 10.5659/AIKAR.2011.13.1.25

Abstract The purpose of this research is to investigate the effect of specific hydration reaction on the stiffening process of cement paste. The cement compositions are manipulated to cause specific hydration reactions (secondary gypsum and syngenite formation) responsible for false set, and the relationship between specific hydration reactions and the flow and stiffening behavior of cement paste were investigated using modified ASTM C 403 penetration resistance measurement and oscillatory shear rheology. X-ray powder diffraction (XRD) was used for the phase identification associated with premature stiffening of cement paste. Differential thermal analysis (DTA) and thermogravimetric analysis (TGA) were used for verification of syngenite formation. From the results, both secondary gypsum and syngenite formation caused faster stiffening and set. The amount of syngenite produced during 1 hour hydration was approximately 1 % of total mass of the cement paste, but cement paste with syngenite formation showed significantly accelerated stiffening behavior compared to normal cement paste.

Keywords : Penetration Resistance, Syngenite Formation, Secondary Gypsum Formation, False Set, Cement Paste

1. INTRODUCTION

The stiffening of cement paste depends on various factors such as the flow behavior of liquid suspensions, in addition to the chemical compositions affecting ionic dissolution and hydration of cement paste. Since net zeta potential of cement particles is slightly negative when mixed with water (Suzuki et al. 1981), the particle interaction is governed by Van der Waals interaction, causing adjacent particles to attract each other. Considering the volume fraction of cement particles in normal w/c ranges, cement paste is known to flocculate without the presence of dispersing agents (Struble et al. 1995). The particle interaction becomes stronger as a result of hydration such as the growth in particle size due to C-S-H formation, increase in

ionic strength, etc.

Generally, the stiffening of cement paste is mainly affected by the hydration of C_3S (Taylor 1997). However, premature stiffening is different from ordinary stiffening because it not associated with interaction between each particle. It is associated with hydration product with specific morphology that affects the flow of cement paste (Taylor 1997). Premature stiffening occurs prior to initial set, mostly during mixing of the cement paste.

Flash set and false set are known as premature stiffening. Flash set is caused by rapid AFm formation (hydroxyl AFm), due to the absence of sulfate at the time of reaction (Taylor 1997, Mindess et al. 2003), whereas false set is caused by secondary gypsum or syngenite formation (Taylor 1997, Mindess et al. 2003). Flash set can be prevented by addition of calcium sulfate phases during grinding process.

However, excessive temperature rise during grinding process is often observed. When the temperature in the mill reaches above 110°C, some gypsum dehydrates and is transformed into calcium sulfate hemihydrate. In order to control the hydration of highly reactive C_3A , this conversion is favorable, because the rate of dissolution of SO_4^{2-} ions is much faster (approximately three times) for calcium sulfate hemihydrate than for gypsum (Aitcin 1998). However, in most cases, this conversion is not favorable because calcium sulfate polymorphs have the same final solubility when they are dissolved in water. Therefore, if sulfate ions are not consumed rapidly, they reach the maximum allowable concentration level and start to precipitate by consuming calcium, sulfate, and water to form secondary gypsum. Stiffening is associated with interlocking of particles caused by the needle-like gypsum crystals in addition to

Corresponding Author: Jae-Yong Lee, Professor

Department of Architectural Engineering, Pukyong National University
Yongdangdong, Namgu, Busan, 608-739, Korea

Tel :+82 51 629 6092 e-mail: jylee@pknu.ac.kr

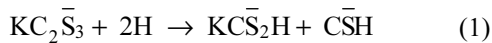
This research was supported by Cemex, USA, when the first author was a research assistant in University of Illinois at Urbana Champaign. The authors deeply appreciate Professor Leslie J. Struble for her guidance and discussions regarding this project, especially for her kind agreement for this manuscript to be submitted to Journal of the Architectural Institute of Korea.

This is an Open Access article distributed under the terms of the Creative Commons Attribution NonCommercial License (<http://creativecommons.org/licenses/bync/3.0/>) which permits unrestricted noncommercial use, distribution, and reproduction in any medium, provided the original work is properly cited.

the reduction in water content. Unlike flash set, the rigidity can be overcome and plasticity can be regained by further mixing without adding water (Mindess et al. 2003). The subsequent strength development is not affected.

The other type of false set (syngenite formation) is associated with alkali sulfates in the clinker. During the clinkering process, when the amount of sulfate is insufficient, the Na_2O (N) enters C_3A and forms less reactive orthorhombic aluminate phase (NC_8A_3) (Taylor 1997). This phenomenon occurs when the source of the fuel for clinkering process is pure and contains relatively less amount of sulfate. However, many cement companies recently uses the source of fuel which contains large amount of waste materials, so it is less pure and contains larger amount of sulfates. When the amount of sulfate is sufficient during clinkering process, alkalis and sulfates usually tend to combine and form alkali sulfates, such as arcanite (KS), thenardite (NS), apthitalite ((K,N)S), and calcium langbeinite (KC_2S_3) (Taylor 1997). More reactive cubic aluminate phase (C_3A) generally forms in this case.

Since alkali sulfates are usually very soluble, they rapidly change compositions of pore solution as soon as cement reacts with water. In some cases, sulfates react with calcium ions in the pore solution and gypsum may precipitate to cause false set. It is also possible that syngenite formation occurs from the hydration of calcium langbeinite or reaction with arcanite, gypsum, and water. The reaction stoichiometry is presented in equations (1) and (2):



Syngenite formation is often observed as a form of pack set* during storage in the silo, but it can be also observed from cement hydration. Formation of syngenite during hydration often leads to false set due to its characteristic of needle-like crystal morphology that interlocks cement particles.

The stiffening of cement paste can be measured using various techniques. One technique, the most commonly used, is simply called the Vicat test (ASTM C 191). However, Vicat test only measures setting time of the cement paste. It is generally understood that this technique is crude, uses stiff dough, which is not a typical fluid cement paste, and gives almost no information on the gradual development of microstructure due to hydration. Therefore, this research attempts to use more sensitive oscillatory shear rheology technique to monitor the premature stiffening of fresh cement paste. The oscillatory shear rheology technique has been successfully used to study aggregated suspensions (Chen 1991, Channell et al. 1997, Channell et al. 2000), and has been successfully used to explore the microstructural development of flocculated cement paste (Lei et al. 1997, Zhang 2001). However, due to the practical stress capacity of oscillatory shear rheometer, modified penetration resistance measurements (ASTM C 403) is also used to monitor stiffening behavior of cement paste. The

* Pack set is often observed when discharging cement from the silo. A huge chunk of cement is formed, which makes it difficult discharge. This is believed to occur with the reaction between calcium langbeinite and moisture in the air.

validity of penetration resistance measurement for monitoring stiffening of cement paste has been well presented by Struble et al.(2001), and successfully modified for stiffening measurement of cement paste (Chung et al. 2010).

This research focuses on systematic investigation regarding the flow and stiffening behavior of cement paste associated with premature stiffening, especially by false set. Cements are properly synthesized to produce hydration phases such as secondary gypsum and syngenite, the stiffening behavior of fresh cement paste are measured, and hydrated phases responsible for premature stiffening are identified using X-ray powder diffraction (XRD) analysis. Differential thermal analysis (DTA) and thermogravimetric analysis (TGA) are also used to complement XRD results for syngenite identification.

2. EXPERIMENTAL PROCEDURE

(1) Material

In order to investigate the effect of premature stiffening on the flow behavior of cement paste, the testing cements are properly treated and synthesized. Two ASTM type I cements were selected for the experiments, one with high in alkali sulfate and one with low in alkali sulfate. The chemical compositions of two type I Portland cements are presented in Table 1. To create secondary gypsum formation, high and low alkali sulfate cements were placed in the 150 °C oven for at least two days. In this environment, the gypsum in the cement will undergo dehydration and be converted to calcium sulfate hemihydrate (plaster of Paris).

In order to observe syngenite formation more easily, cement that contains large amount of calcium langbeinite is favorable, as shown in equation (1). However, as shown in equation (2), syngenite formation also occurs with the absence of calcium langbeinite, from reaction with potassium sulfate (arcanite), gypsum, and water. The way to produce syngenite formation is determined after XRD analysis of high alkali sulfate cement. However, low alkali sulfate

Table 1. Chemical compositions of high and low alkali sulfate cement

Compositions	High alkali sulfate cement	Low alkali sulfate cement
SiO_2 (%)	19.44	20.2
Al_2O_3 (%)	5.06	4.8
Fe_2O_3 (%)	2.19	3.4
CaO (%)	62.74	63.3
MgO (%)	3.96	2.4
SO_3 (%)	3.42	3.1
LOI (%)	1.52	1.5
Insoluble residue	0.20	0.35
C_3S	61	67
C_2S	10	7
C_3A	10	7
C_4AF	7	10
Total alkalis*	1.05	0.59

*Total alkali content (Na_2O equivalent content):
 Na_2O content + $0.658 \times \text{K}_2\text{O}$ content

cement was not considered for this experiment because it is less likely to form syngenite without the presence of arcanite or calcium langbeinite in the cement.

(2) X-ray diffraction

The high alkali sulfate cement was analyzed using XRD to determine the presence of any type of calcium sulfate polymorphs and alkali sulfates that may cause premature stiffening. Salicylic acid/methanol (SAM) extraction was used to facilitate identification of C_3A (aluminite), C_4AF (ferrite), and minor phases such as calcium sulfate and alkali sulfates through removal of C_3S (alite), C_2S (belite), and free lime. Hydrated cement pastes were examined using XRD to determine the formation of secondary gypsum and syngenite. The low alkali sulfate cement was also analyzed using XRD to verify the conversion of gypsum to calcium sulfate hemihydrates. SAM extraction was not used with low alkali sulfate cement since the decrease in gypsum peak associated with its dehydration can be easily identified even with the presence of calcium silicate phases.

(2.1) Salicylic acid methanol (SAM) extraction:

The high alkali sulfate cement was extracted using salicylic acid/methanol (SAM). The sample, 5 g of cement or clinker, was added to a solution containing 20 g of salicylic acid in 300 ml methanol and the mixture was stirred for 2 hours. The suspension was vacuum filtered using a Buchner funnel and a filter. The residue was washed with methanol and dried in a 60°C vacuum oven until XRD analysis.

(2.2) Preparation of hydrated cement paste

Cement pastes of w/c 0.4 were prepared at 25 °C laboratory condition by hand mixing of 100 g cement and 40 g nano-pure deionized water that were preconditioned to the laboratory temperature. Mixing was done for 3 minutes by hand with a steel spatula. Pastes were poured into a plastic container, covered by a lid, and then stored at 25 °C. Specimens were taken at 5 (after mix) minute, 1 hour, 2 hour and 3 hour. Immediately after collection, specimens were placed in a 20-ml glass vial, filled approximately one-third with paste, and methanol was added to stop hydration, shaking to dilute the water. The cement paste was allowed to settle, the methanol-water liquid was carefully removed by pipette, fresh methanol was added, and sample was shaken. This sample was stored for a few hours, and the liquid layer was again removed by pipette. Fresh methanol was added a third time, and the sample was stored until analysis began. Before XRD analysis, the methanol was removed by pipetting.

(2.3) XRD testing

Prior to XRD testing, hydrated specimens were mixed with acetone and the resulting slurry was ground in a mortar and pestle to a particle size of approximately 10 μm , then the acetone was

evaporated. Prepared samples were packed into the container, and the sample container was then placed in the Rigaku Geigerflex D/Max-VB x-ray diffractometer. Scanned 2-theta angle was from 5° (2 θ) to 70° with a step size of 0.02° and a dwell time of 1.5 seconds. The working voltage was 40 kV and the electric current was 40 mA. The same setup was used for the analysis of unhydrated cement. Computer programs were used to perform the XRD scans and to assist the data analyses* .

(3) Thermal analysis

It is often difficult to distinguish the syngenite and ettringite in cements paste using XRD since the characteristic peaks of two phases are very close to each other. In addition, phase compositions of cement are so complicated that other peak angles are not clearly represented. Thus, thermal analysis was used to verify the syngenite formation. The amount of sample for thermal analysis was approximately 20 mg. Sample for thermal analysis was exactly the same sample which was previously analyzed by XRD. After XRD, sample was stored in vacuum desiccator with dry-rites to prevent further hydration. DTA (differential thermal analysis) – TGA (thermogravimetric analysis) sample holder was placed at Netzsch STA-409 thermal analysis equipment. Air was constantly supplied during the test. Heating rate was 10°C/min with temperature range of 25 ~ 1000 °C.

(4) Penetration resistance

Modified ASTM C 403 penetration resistance (Chung et al. 2010) test was performed at selected time intervals on samples that were hydrated in the laboratory at 25 °C. Cement pastes of w/c 0.4 were prepared by mixing 1500 g cement and 600 g water using a Hobart paddle mixer. Temperature of the laboratory and the mixing water was maintained at 25 °C. Mixing was performed following ASTM C 305 with slight modification in procedure. Paste was first mixed for 30 seconds at the lowest speed level (140±5 rpm). The mixer was stopped for 30 seconds to 60 seconds in order to scrape down cement paste adhering to the side of the mixing bowl. As soon as scraping was finished, the paste was mixed for 90 seconds at the intermediate speed level (285±10 rpm).

As soon as the cement paste was mixed, it was placed at 150 mm × 150 mm × 100 mm plastic container, covered with a plastic Wrap to prevent evaporation, and stored at 25°C testing laboratory. Prior to each penetration, bleed water was removed. Penetrations were measured using an Instron 4500 testing apparatus, equipped with the proper Proctor needles. A 1 kN load cell was used. Measurements were made in triplicate and averaged. Measurements were first made at 2 hour. Each measurement was measured at 1-hour intervals up to initial set and 30-minute intervals after initial set. To calculate penetration resistance, load required to penetrate 25 mm depth was divided by area of the needle that is used at each measurement.

(5) Oscillatory shear rheology (dynamic rheology)

A Bohlin CS rheometer, operated using stress controlled dynamic oscillatory shear was used for the experiment. However, cements used in this experiment showed such a high initial stiffness that tests (modulus vs. stress) cannot be performed with the same w/c (0.4), the measurements were performed at w/c 0.45. It should be

* For operating and collecting XRD scanning data, the MDI Datascan was used. For XRD analysis, the MDI JADE was used. MDI JADE automatically finds the phases present in the sample from raw XRD data by comparing characteristic peaks. The time required for identifying phases was significantly reduced with this program.

noted that the use of superplasticizer is never been considered for the experiment. The main reason is to avoid problem associated with interaction between cement paste and superplasticizer that may cause abnormal stiffening. Another reason is that the use of superplasticizer blurs the effect of premature stiffening because of its dispersing ability.

The cement paste was prepared by hand mixing for 3 minutes using 10 g cement and 4.5 g water. Mixed cement pastes were then poured into the sample cup and the bob was lowered into place. In order to eliminate any effect of hand mixing and to provide a uniform starting condition, pastes were presheared in the rheometer at 200 Pa for 45 seconds and then allowed to equilibrate for 300 seconds. Oscillation stress was then applied at a frequency of 1 Hz and a sequence of increasing amplitude.

Rheological measurements were performed at selected time intervals such as 5 minute, 30 minute, and 1 hour at 25 °C. Temperature was maintained using water circulating through the cup from a temperature-controlled bath. Several types of geometry are available for rheological measurements, but the couvette geometry (C14 bob and cup which are generally used for other colloidal suspensions) was selected. The C14 bob has a diameter of 14 mm. The gap between the bob and cup is 0.7 mm.

3. RESULTS AND DISCUSSION

(1) High alkali sulfate cement

In Figure 1 and 2, XRD patterns of the high alkali sulfate cement before and after SAM extraction are presented.

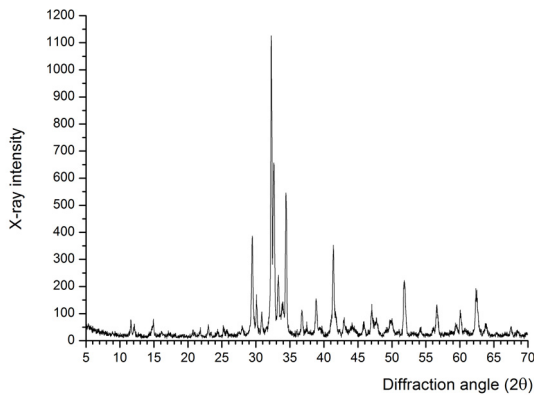


Figure 1. XRD pattern of high alkali sulfate cement

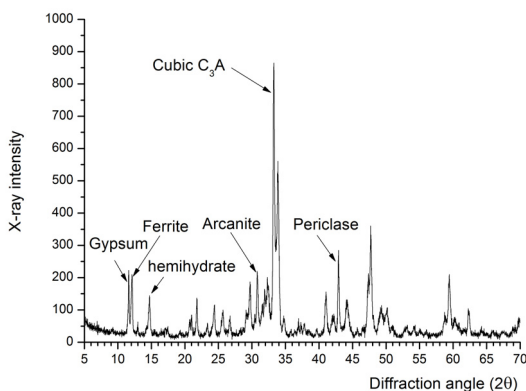


Figure 2. XRD pattern of high alkali sulfate cement after SAM extraction

From Figure 2, high alkali sulfate cement showed two forms of calcium sulfates, gypsum and the hemihydrate. The presence of hemihydrate indicates the possibility of secondary gypsum formation. The cement also contained arcanite, but no calcium langbeinite was observed. In order to observe syngenite formation more easily, cement that contains large amount of calcium langbeinite is favorable, as shown in equation (1). However, since there is no calcium langbeinite present in the high alkali sulfate cement, 2% K_2SO_4 was added to the base cement to produce equation (2) type syngenite formation.

(2) Hydration of high alkali sulfate cement

Figure 3 shows XRD patterns of hydrated high alkali sulfate cement pastes at each time period. Compare to the unhydrated high alkali sulfate cement shown in Figure 1, the relative X-ray intensity of gypsum peak has shown to increase (from 77 to 159). This can be an evidence of secondary gypsum formation. However, the cement paste did not show significant stiffening by eye observation. Ettringite was observed during all of the selected hydration period, and syngenite formation was not clearly identified.

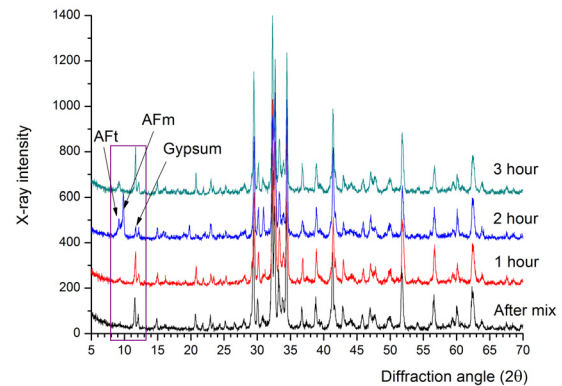


Figure 3. XRD pattern of hydrated high alkali sulfate cement

The interesting finding from this result is that AFm peak was observed at 2 hour and disappeared at 3 hour. The high alkali sulfate cement paste showed transient formation of AFm. Generally, transient formation of AFm is an unusual phenomenon to observe. The possible cause is not well understood, but there are two possible reasons that may explain this phenomenon. One is that AFm phase became less crystalline and was not detected by XRD at certain time, becoming so-called XRD amorphous condition. However, the other reason can explain this phenomenon even better that the amounts of sulfate and C_3A are out of balance at that critical time as shown in Figure 3. The intensity of gypsum peak maintained constant for all hydration period, except for 2 hour hydration which showed significant decreased in its intensity. This finding corresponded well with sudden increase in AFm peak intensity at 2 hour. At 2 hour, the high alkali sulfate cement showed AFm peak along with ettringite peak. The high alkali sulfate cement seems to show very unstable hydration kinetics during first three hours.

(3) Secondary gypsum formation

Figure 4, 5, and 6 shows the XRD patterns, oscillatory shear rheology results, and penetration resistance results of hydrated

high alkali cement paste that was heated in 150°C oven for two days. According to the XRD analysis shown in Figure 4, ettringite formation was observed for all periods. However, no gypsum peak was observed the cement paste after mix. This can only be explained that there is not enough time for calcium ion and sulfates to fully precipitate when hydration was stopped after mix. However, this result also indicates that all the gypsum in the high alkali sulfate cement has been successfully transformed into hemihydrate. At 30 minutes and 1 hour, gypsum was observed as a result of secondary gypsum formation.

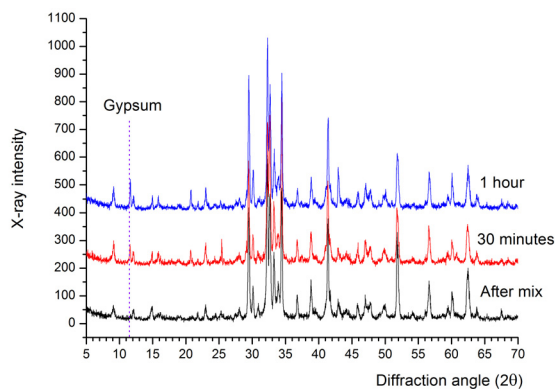


Figure 4. XRD pattern of hydrated high alkali sulfate cement heated at 150°C (cement forming secondary gypsum)

From oscillatory shear rheology results shown in Figure 5, heated cement paste showed higher yield stress up to 1 hour. The difference in yield stress (the stress level where significant drop in storage modulus is observed) was the largest right after mixing, but the difference started to decrease from this period and minimized at 1 hour. The increased yield stress can be due to secondary gypsum formation.

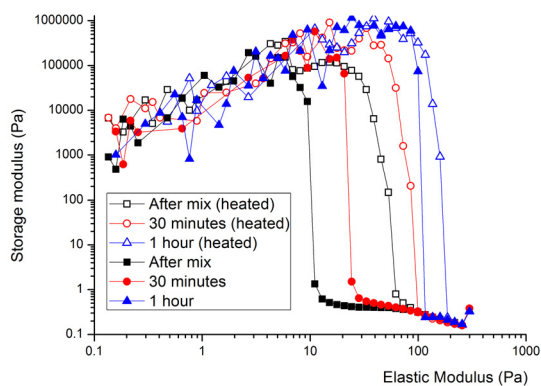


Figure 5. Oscillatory shear rheology of high alkali sulfate cement paste

In Figure 6, penetration resistance data of heated and unheated high alkali sulfate cements are presented. Heated high alkali cement showed slightly faster stiffening at early hydration period (although it is not notable from Figure 6) compared with base cement. However, the difference is very small between these two cement

pastes. The effect of secondary gypsum formation by penetration resistance measurement was not evident. This seems to be mostly associated with the presence of calcium sulfate hemihydrates with unheated high alkali sulfate cement (Figure 2). It is possible to speculate that the recrystallization of gypsum did not bring significant difference on the flow behavior of the cement paste because the unheated cement paste already showed some level of secondary gypsum formation.

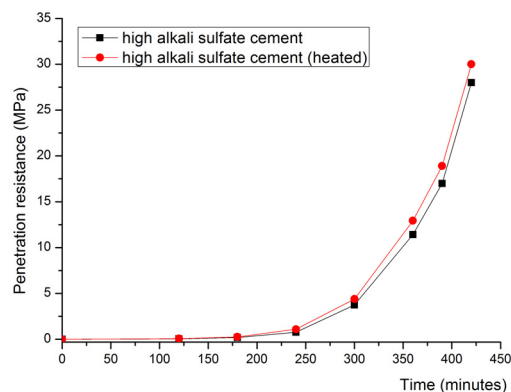


Figure 6. Penetration resistance of high alkali sulfate cement paste

Therefore, further investigation was done using different type of cement, which is low alkali sulfate cement, and penetration resistance was measured. In low alkali sulfate cement, most of the sulfates are in the form of calcium sulfate polymorphs ($\text{CaSO}_4 \cdot x\text{H}_2\text{O}$), not in the form of alkali sulfates as shown in Figure 7. The cubic type C_3A was observed, and gypsum peak was disappeared after heating the cement at 150°C oven for two days.

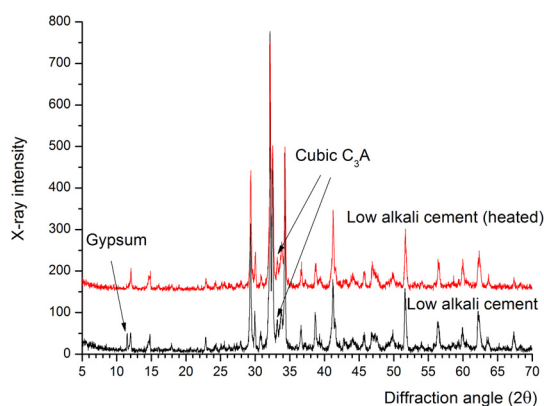


Figure 7. XRD pattern of heated and unheated low alkali cement

Figure 8 presents the stiffening behavior of the heated and unheated low alkali cement. The secondary gypsum formation produced by low alkali cement showed faster stiffening and setting up to final set. This is opposite to what was observed from Figure 6. In addition, it is shown from Figure 9 (Figure 9 presents the blue rectangle area of Figure 8.) that there is a sudden increase in initial stiffness during 1 hour. The heated low alkali cement showed penetration resistance of 0.32 MPa and unheated low alkali cement showed penetration resistance of 0.01 MPa. It is believed that the

initial change in the paste microstructure due to recrystallization of gypsum has affected the whole stiffening behavior of cement paste. It was also found that earlier microstructural changes could be crucial to the later setting and hardening behavior.

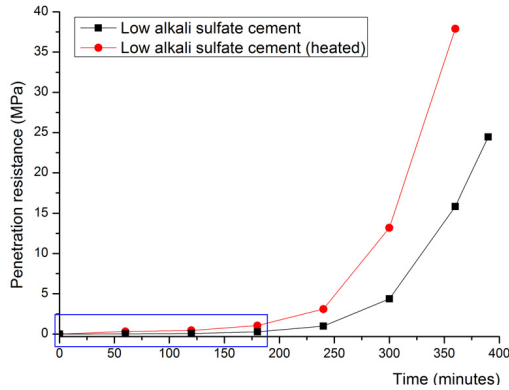


Figure 8. Penetration resistance of low alkali sulfate cement paste

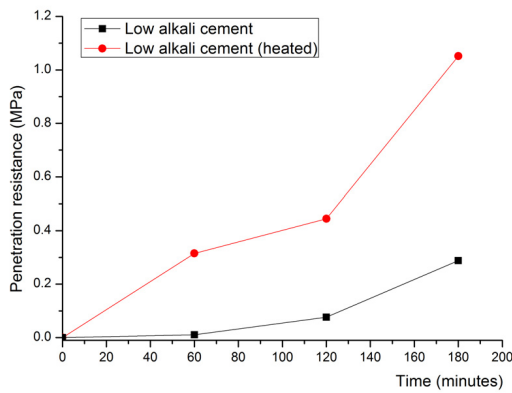


Figure 9. Penetration resistance of low alkali sulfate cement paste. Note that blue rectangle region in Fig. 8 is replotted.

As noted, the result from low alkali sulfate cement is quite different from what was observed with the high alkali sulfate cement. It seems that the effect of false set to the flow behavior can be dependent upon the chemical compositions of cement. However, at least, both cements showed faster stiffening at early hydration period. This finding coincides with the eye observation that the heated cement paste showed stiffer behavior during mixing and thus was more difficult to pour those cement pastes into test container for penetration resistance.

(4) Syngenite formation

Figure 10 presents hydrated high alkali sulfate cement paste with addition of 2% K_2SO_4 . For better identification of ettringite and syngenite peaks, Figure 11 is replotted focusing on 5 to 25° 2 theta area presented in Figure 10. From Figure 11, XRD results show a weak gypsum peak, and a modest ettringite or syngenite peak. However, this peak near 9° 2θ is shown to be more like a broad peak instead of sharp peak at each diffraction angle since the characteristic peaks of ettringite and syngenite are located at 9.091° 2θ and 9.312° 2θ, respectively. As already mentioned, the syngenite

peak can be sometimes misinterpreted as an ettringite peak. Comparing other peaks of ettringite and syngenite are also difficult due to the similarity of the patterns, the width of these low intensity peaks, and the complicated pattern of cement paste. Therefore, the result may indicate the presence of both ettringite and syngenite. In order to clarify this question, DTA and TGA were carried out on this sample to help differentiate these two phases.

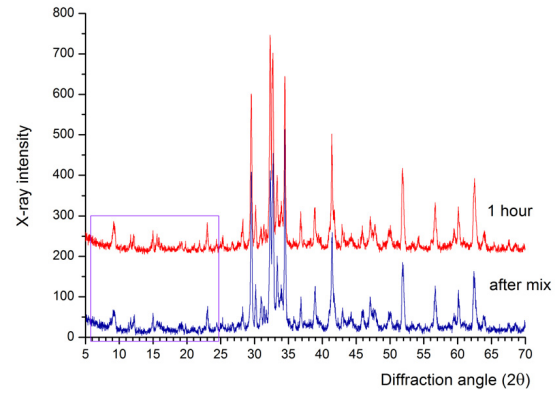


Figure 10. XRD pattern of hydrated base cement with addition of 2% K_2SO_4

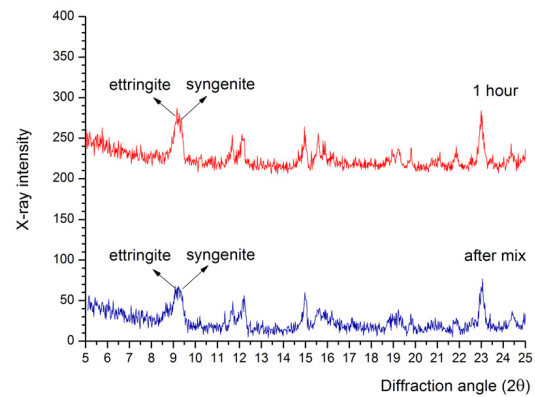


Figure 11. XRD pattern of hydrated base cement with addition of 2% K_2SO_4 . Note that purple square area in Fig. 10 is replotted.

According to the DTA results shown in Figure 12, a distinctive thermal activity was observed at 273°C and 733°C and a small thermal activity was observed at 128°C. The peak at 128°C could be due to C-S-H, or ettringite, since ettringite has a thermal peak around 135~140°C and C-S-H has a thermal peak around 115~125°C (Taylor 1997). The thermal peak at 273°C is attributed to syngenite decomposition, which is known to occur around 250~300°C (Taylor 1997). The peak at 733°C was attributed to decomposition of calcium carbonate ($CaCO_3$), which occurs at a wide range of temperature, 500~800°C. TGA results shown in Figure 12 correspond to the DTA results. It was found from TGA that the amount of syngenite formed during the 1 hour hydration was about 1% by weight of the sample. The thermal analysis results provides strong evidence that syngenite was formed by addition of potassium sulfate, although samples may contain some ettringite as well.

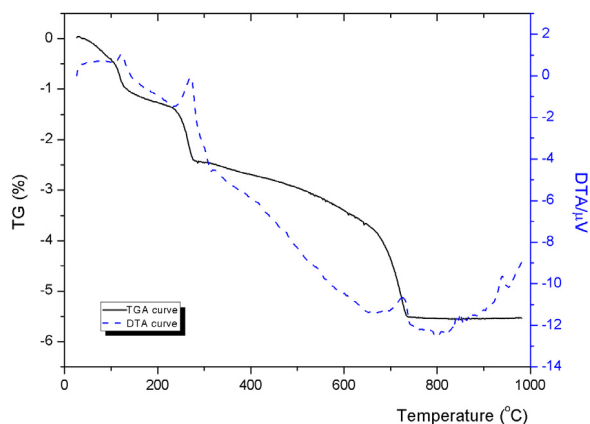


Figure 12. DTA and TGA response of cement forming syngenite

Figure 13 presents stiffening behavior of high alkali sulfate cement paste and cement paste that exhibits syngenite formation. It was observed that syngenite formation significantly accelerated overall stiffening. With 2% K_2SO_4 addition, the cement paste was stiff at the beginning of the mixing period, and showed very rapid stiffening with moderate heat evolution. The flocculation caused was so strong, and the mixture became so sticky, that the paste did not flow even when the paste container was overturned. It was possible to break down the structure by stirring or by tapping the container, but the paste was still very stiff (high in viscosity). Immediately after breaking down the solid structure, the cement paste got back to its original shape by tapping the container, indicating a highly thixotropic response. It should be noted that specimen was also prepared for oscillatory shear rheology measurement, but it was unable to perform rheological measurement simply because the mixture actually passed stress limit of the rheometer even in w/c of 0.45.

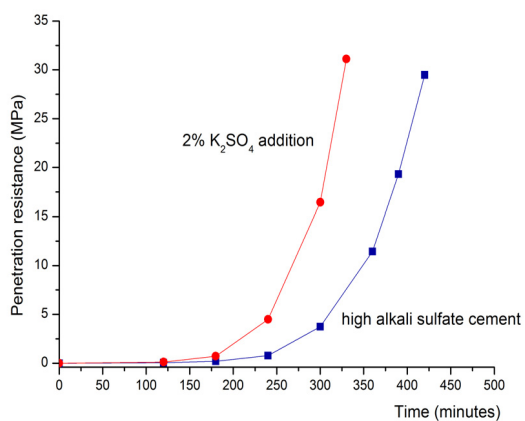


Figure 13. Penetration resistance of high alkali sulfate cement and high alkali sulfate cement with 2% K_2SO_4 addition

From the penetration resistance measurements of cement paste with syngenite formation, not only the higher penetration resistance was observed at the beginning, but also higher penetration resistance was maintained up to final set. This follows

well with classical description of false set (Taylor 1997, Mindess et al. 2003). Although the results suggests that syngenite formation showed classical false set type response, but visual observation suggests that the degree of stiffness is more close to that of flash set. It is interesting to mention that such a significant acceleration in stiffening was caused by only 1% syngenite formation.

4. FUTURE WORK

The definition of false set is a rapid set without a large heat evolution, in which plasticity is regained on further mixing and subsequent strength development is not markedly affected. In this research, false set was produced by secondary gypsum and syngenite formation. False set was expected to accelerate overall stiffening process of cement paste in addition to its earlier increase in the yield stress.

According to the test results shown, false set generally caused severe changes in its stiffening characteristic. Because the set is caused by the needle-like crystal structure of gypsum and syngenite and their interlocking capability of cement particles, the amount of secondary gypsum and syngenite produced during hydration may determine the stiffening characteristic. However, it should be noted that it is difficult to correlate the X-ray intensity to the amount of secondary gypsum and syngenite because those two phases has such a high preferred orientation. Even though one can successfully estimate the amount of each phase by quantitative Rietveld analysis, it is still difficult to determine that the amount is a single major factor governing the degree of premature stiffening since the degree of premature stiffening can be also determined by several other factors such as 1) where the gypsum or syngenite is formed (the location), 2) how effectively gypsum or syngenite interlocks each cement particles, and 3) what the morphology of gypsum or syngenite is (the aspect ratio). The morphology of gypsum can be altered by space availability for crystal growth. Thus, it may be affected by other hydration constituents such as C-S-H barrier around the calcium silicate particles or ettringite barriers near C_3A particles, which makes more difficult to understand this phenomenon. It should be noted the relationship between those properties to the stiffening behavior of the cement paste should be investigated in order for better understanding of premature stiffening mechanism.

5. CONCLUSIONS

According to the experimental findings in this study, following conclusions can be drawn.

- 1) Both secondary gypsum and syngenite formation caused faster stiffening and set.
- 2) The effect of secondary gypsum formation was seen to vary according to the chemical composition of cement.
- 3) Syngenite was produced with the addition of 2% K_2SO_4 to base cement. Syngenite formation caused so much rapid stiffening that the paste could not be tested with the oscillatory shear rheometer, and significantly faster stiffening and set with the penetration resistance test.
- 4) The amount of syngenite formed during 1 hour of hydration is approximately 1% by weight of cement paste.

REFERENCES

- Aitcin, P. C. (1998), High Performance Concrete, E & FN SPON, ASTM Test Method for Time of Setting of Hydraulic Cement by Vicat Needle (C 191), Annual Book of ASTM Standards, Vol. 04. 01, ASTM International, West Conshohocken, PA, 2003.
- ASTM Test Method for Time of Setting of Concrete Mixtures by Penetration Resistance (C 403), Annual Book of ASTM Standards, Vol. 04. 02, ASTM International, West Conshohocken, PA, 2003.
- Channell, G. M., and Zukoski, C. F. (1997), "Shear and Compressive Rheology of Aggregate Alumina Suspensions, AICHE Journal, Vol. 43: 1700-1708.
- Channell, G. M., Miller, K. T., and Zukoski, C. F. (2000), "Effect of Microstructure on the Compressive Yield Stress, AICHE Journal, Vol. 46: 72-78.
- Chen, L. B. (1991), "The Dynamic Properties of Concentrated Charge Stabilized Suspensions". Ph.D dissertation, University of Illinois at Urbana-Champaign, Urbana (IL).
- Chung, C. -W., Mroczek, M., Park, I. -Y., and Struble, L. J. (2010), "On the evaluation of setting time of cement paste based on ASTM C 403 penetration resistance test", Journal of Testing and Evaluation, Vol. 38: 527-533.
- Lei W. G., and Struble. L. J. (1997), "Microstructure and Flow behavior of Fresh Cement Paste," Journal of American Ceramic Society, Vol. 80: 2021-2028.
- Mindess, S., Young, J. F., and Darwin, D. (2003), Concrete, 2nd edition, Prentice Hall.
- Struble, L. J., and Sun, G. - K. (1995), Viscosity of Portland Cement Paste as a Function of Concentration, Advanced Cement Based Materials, Vol. 2: 62-69.
- Struble, L. J., Kim, T.-Y., and Zhang, H., Setting of Cement and Concrete. Journal of Cement, Concrete, and Aggregate, 2001, Vol. 23:
- Suzuki, K., Nichikawa, T., Kato, K., Hayashi, H., and Ito, S. (1981) "Approach by Zeta-Potential Measurement on the Surface Charges of Hydrating C_3S ," Cement and Concrete Research, Vol. 11: 759-764.
- Taylor, H. F. W. (1997), Cement Chemistry, 2nd edition, Academic Press, Thomas Telford edition,
- Zhang, H. (2001), "Using Dynamic Rheology to Explore the Microstructure and Stiffening of Cementitious Mixtures, Ph.D dissertation, University of Illinois at Urbana Champaign, Urbana (IL).

(Date of Submission : 2011.1.6)